NASA Technical Memorandum 78599

Wind-Tunnel Investigation of Highly Maneuverable Supersonic V/STOL Fighter

Michael Falarski

June 1979

NASA
National Aeronautics and
Space Administration

WIND-TUNNEL INVESTIGATION OF HIGHLY MANEUVERABLE SUPERSONIC V/STOL FIGHTER

Michael Falarski

Ames Research Center, NASA
Moffett Field, California 94035

SUMMARY

This paper presents a brief summary of the results from the initial wind-tunnel test of a large-scale, highly maneuverable supersonic V/STOL fighter model in the Ames 40- by 80-Foot Wind Tunnel. The STOL configuration which was tested combines upper surface blowing and spanwise blowing to improve the lift characteristics over a wide angle-of-attack range. A close-coupled canard was added to this configuration to create a highly maneuverable STOL aircraft. The 7.28 m (24 ft) span model is powered by two J-97 turbojet engines, each producing 9340 N (2200 lb) thrust at a pressure ratio of 2.

With the nozzle flap and aileron set at 30°, the model produced lift coefficients greater than 4. The model was longitudinally unstable because of the forward canard position and because of the large body area of fuselage, strake, and nacelles forward of the center of gravity. The canard had a positive interference effect on both lift and drag but was limited in its control effectiveness by stall. Spanwise blowing delayed wing stall and increased the linear portion of the lift curve. It did not significantly increase maximum lift, however, because of body stall.

INTRODUCTION

In recent years, interest in military application of V/STOL technology has revived, especially regarding the development of a highly maneuverable, supersonic fighter aircraft. Recent aircraft design studies (ref. 1) have detailed areas where technological uncertainties still exist which will impede the development of a V/STOL aircraft. Because the takeoff and approach performance is one of these areas of uncertainty, Ames has designed and fabricated a large-scale wind-tunnel model of a V/STOL fighter to study low-speed aircraft characteristics. This model can be adapted to different V/STOL propulsion concepts.

This paper presents a brief summary of the results from the initial wind-tunnel test of this model adapted to the upper surface blowing propulsion concept. This is combined with spanwise blowing (SWB) and closed-coupled canards to augment the lift over a wide angle-of-attack range. Results of wind-tunnel tests of a similar small-scale model (refs. 2-3) have shown that this combination produces a highly maneuverable STOL concept.

The complete model description and analysis of all the wind-tunnel results will be published at a later date in a NASA Technical Memorandum.

SYMBOLS

b wing span, m (ft)

C_d drag coefficient, $\frac{\text{drag}}{qs}$

C_L lift coefficient, $\frac{\text{lift}}{qs}$

C_{L_Γ} circulation lift coefficient, $\frac{\text{circulation lift}}{qs}$

C_ℓ roll moment coefficient, $\frac{\text{roll moment}}{qs\ b}$

C_{ℓ_β} rate of change of C_ℓ with β

$C_{m_{LE}}$ pitching-moment coefficient, $\frac{\text{pitching moment}}{qS\bar{c}}$

C_n yawing-moment coefficient, $\frac{\text{yawing moment}}{qs\ b}$

C_{n_β} rate of change of C_n with β

C_T thrust coefficient, $\frac{\text{total axial gross thrust}}{qs}$

C_Y side-force coefficient, $\frac{\text{side force}}{qs}$

C_{Y_β} rate of changes of C_Y with β

c local wind chord, m (ft)

$\bar{c}$ mean aerodynamic chord, m (ft)

q wind-tunnel free-stream dynamic pressure, n/m (lb/ft)

S wing reference area, m (ft)

α wing angle of attack, deg

β sideslip angle, deg

δ_a aileron deflection angle ref. to aileron centerline, deg

δ_c canard deflection angle, deg

δ_f nozzle flap deflection angle ref. to flap centerline, deg

Note: All moments referenced to leading edge of $\bar{c}$. Forces are wind axes and moments are stability axes.

MODEL AND TEST DESCRIPTION

The V/STOL fighter model is shown installed in the test section of the Ames 40- by 80-Foot Wind Tunnel in figure 1. A sketch of the overall model and propulsion system geometries are presented in figure 2. The model is approximately 0.7 scale incorporating a 40° swept wing with pitching moment control provided by a close-coupled canard and beaver tail. For this investigation the canard was mounted in the forward position of the three available longitudinal canard positions. Limited test time did not allow for the investigation of the canard leading- and trailing-edge flaps nor the beaver tail.

The model is powered by two J-97 turbojet engines mounted in nacelles at 0.33 b/2 to provide a strake between the fuselage and nacelles for future integration of a VTOL ejector propulsion system. The engine exhaust is pre-turned to 25° by the aspect ratio = 8, two-dimensional wedge nozzle. It is blown over the upper surface of the nozzle flap. The nozzle flap is capable of vectoring the exhaust from -10° to +30°. When tests were made with SWB, the flap nozzle area is reduced 17% and the SWB nozzle uncovered. The SWB nozzle is mounted flush with the outboard nacelle wall at 23% of the wing root chord. Both a circular and an aspect ratio = 4 rectangular nozzle have been designed for the model. The rectangular nozzle was used for this investigation.

The model has been instrumented to measure: canard, strake, wing, and beaver-tail surface pressures; wing- and beaver-tail surface temperatures; exhaust total pressure distribution at nozzle exit and flap trailing edge; and engine duct flow properties before and after the SWB nozzle station. The surface instrumentation is located on the model's left side and can be seen in figure 1 as the unpainted strips.

The model was investigated through angle of attack and sideslip ranges of -8° to +40° and -10° to +30°, respectively, and thrust coefficients of approximately 0 to 2.0. The engines were operated at exhaust total pressure ratios of 1.8 and 2.0. Most of the data were taken at 2.0 which produces a thrust per engine of 9341 N (2200 lb) and an exhaust temperature of 1100° F. The model is now undergoing a static thrust calibration to determine exact thrust coefficients.

RESULTS AND DISCUSSION

The principal objective of this first wind-tunnel test was to investigate the longitudinal aerodynamics of the basic V/STOL fighter configuration, and to briefly sample the canard and SWB effects and lateral-directional characteristics. The longitudinal results will be discussed first in detail followed by a brief discussion of the lateral-directional data. The model data matrix will be completed with two additional wind-tunnel entries in 1979.

Basic Model Longitudinal Characteristics

The longitudinal characteristics of the model with the nozzle flap and aileron set at 30° and the canard at 0° is presented in figure 3. The lift curve slope is linear up to $\alpha = 15°$ where the wing stalls. The lift continues to increase after the wing stalls because of the lift generated by the body consisting of the strake, fuselage, and nacelles. Power increased $C_{L_{MAX}}$ and α_{STALL} but had little effect on the lift curve slope. The $C_{L_{MAX}} > 4$ were achieved with $C_T = 2$.

The model pitching moment has been referenced to the leading edge of the mean aerodynamic chord, $\bar{c}$, which design studies have shown to be a reasonable location of the aircraft center of gravity. With this moment reference the model is longitudinally unstable with a negative static margin of >0.40. Power does not change the margin but does produce large negative moment shifts. This large instability results from the lift generated by the canard, strake, nacelle, and fuselage forward of the reference. Moving the canard to the aft position will relieve this instability but may not reduce it to the -0.15 to -0.20 static margin desirable for modern aircraft control systems.

Canard Effects

The effect of canard presence and its deflection are presented in figures 4 and 5, respectively. The canard has a favorable effect on both lift

and drag. Wing stall is delayed and $C_{L_{MAX}}$ increased by approximately 0.3. Drag is reduced over the entire lift range with the effect larger at the high lifts. The principal adverse effect is the increased longitudinal instability. Moving the canard aft would reduce this instability. This configuration will be investigated during the next wind-tunnel test.

The canard was effective in controlling pitching moment up to a combined canard deflection and angle of attack of 24°. Above 24° the canard stalled and the pitching moment returned to the undeflected valve. The use of the canard leading edge to delay stall and extend the canard usefulness will be investigated during the next test.

Nozzle Flap Effects

The data discussed up to now have been for a nozzle flap deflection of 30°. A limited amount of data was also recorded at a deflection of 0°. In both cases the aileron were deflected to the same angle as the nozzle flap. A comparison of the two flap deflections with the canard removed is presented in figure 6. Reducing the flap deflection reduced the lift at a constant angle of attack and delayed stall allowing almost the same maximum lift to be achieved. Drag was reduced at low lifts and increased at the high lift. This flap change also produced a large positive shift in the zero-lift pitching moment.

Spanwise Blowing (SWB) Effects

The upper surface blowing concept is designed to enhance aircraft lift over a wide range of α by combining the jet flap effect to induce circulation lift, and vortex augmentation to delay wing stall. The jet flap effect is created by the two-dimensional nozzle/flap, while the vortex augmentation is provided by the SWB. The SWB delays wing leading-edge vortex breakdown delaying wing stall (ref. 4). The SWB for the fighter model is provided by diverting 17% of the J-97 exhaust to a rectangular nozzle mounted flush with the outboard nacelle wall at 23% of the wing root chord. As can be seen in figure 7, SWB did delay stall and increased lift at the high α. The maximum lift and model stall were not significantly altered because they are controlled by body stall. SWB also reduced drag and pitching moment at the high lifts. All of these effects were much more pronounced at the high thrust coefficients.

To assist in understanding of the SWB effects, the wing surface pressures and temperatures are being analyzed. A typical example of these data is presented in figures 8 and 9. These data show SWB to significantly increase both the aerodynamic load and temperature at the wing tip. The temperature data were severely limited by premature failure of the thermocouple probes resulting from the adverse flow environment. These probes will be modified for future tests, and several dynamic transducers will be installed in the wing to measure pressure fluctuations. The SWB data are still being analyzed, but initial results indicate that incorporation of SWB into an aircraft will necessitate change in the wing structure to cope with the pressure and temperature environment.

Circulation Lift

As previously indicated the model is designed to provide flow circulation to enhance the aircraft lift. The model circulation lift, C_{L_Γ}, at $\alpha = 0$ with and without SWB is presented in figure 10. The upper surface blowing does benefit from circulation lift and SWB increases it even further. The C_{L_Γ} can amount to 15 to 30% of the total lift depending on the thrust coefficient and the SWB. Without SWB the C_{L_Γ} increases very slowly above $C_T = 0.8$, while with SWB operation C_L continues to increase as a result of increased circulation around the wing.

Lateral-Direction Characteristics

The limited lateral-directional data recorded during this first test indicate no unusual characteristics (figs. 11-12). The basic model, with the flaps and aileron deflected to 30°, and the canard at 0°, shows positive side force and lateral stability. It also shows neutral to slightly unstable directional stability at low α and β. Power has a small effect on the lateral and directional stability. Angle of attack has a destabilizing effect on the lateral stability while increasing directional stability. SWB had only small effects on the lateral-directional characteristics.

CONCLUSIONS

The following general conclusions can be drawn from the results of the initial investigation of the fighter model:

1. An upper surface blowing concept applied to a V/STOL fighter configuration can produce maximum lift coefficients greater than 4.

2. Lift generated by the canards, strake, and fuselage area forward of the c.g. contributes to static instability, and for the configuration tested, resulted in a large unstable static margin.

3. Canards delay wing stall and reduce drag, but their control effectiveness is limited by stall.

4. The spanwise blowing delayed wing stall but did not significantly increase maximum lift because maximum lift is controlled by body stall.

5. At $\alpha = 0°$, the upper surface blowing induces circulation lift that is about 15 to 20% of the total lift.

REFERENCES

1. Lummus, J. R.: Study of Aerodynamic Technology for a V/STOL Fighter/ Attack Aircraft. NASA CR-152128, 1978.

2. Whitten, Perry D.: An Experimental Investigation of a Vectored-Engine-Over-Wing Powered-Lift Concept. AFFDL-TR-76-92, 1978.

3. Bradley, R. G.; Jeffries, R. R.; and Capone. F. J.: A Vectored-Engine-Over-Wing Propulsive-Lift Concept. AIAA Paper 97-917, Sept. 1976.

4. Bradley, R. G.; and Wray, W. O.: A Conceptual Study of Leading-Edge Vortex Enhancement by Blowing. AIAA J. of Aircraft, vol. II, Jan. 1974.

(a) 3/4 rear view.

Figure 1.- V/STOL fighter model installed in wind tunnel.

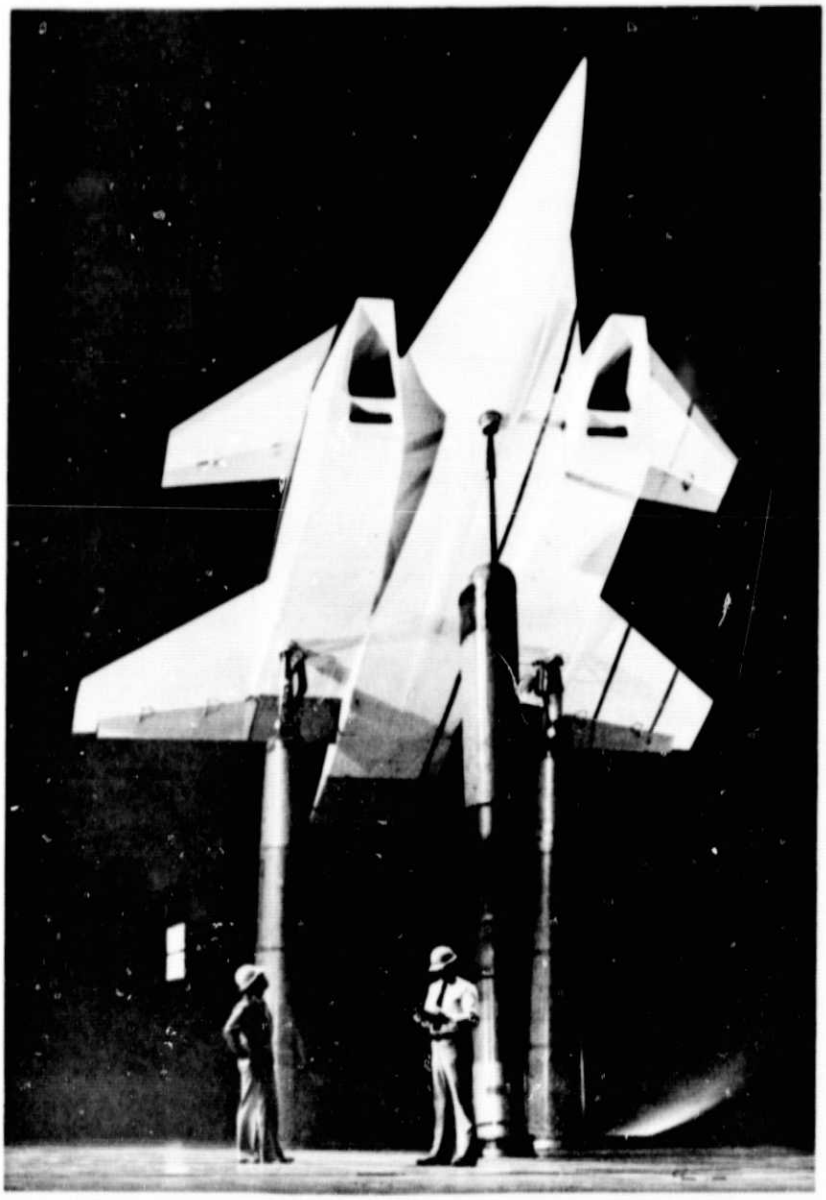

(b) 3/4 front view.

Figure 1.- Concluded.

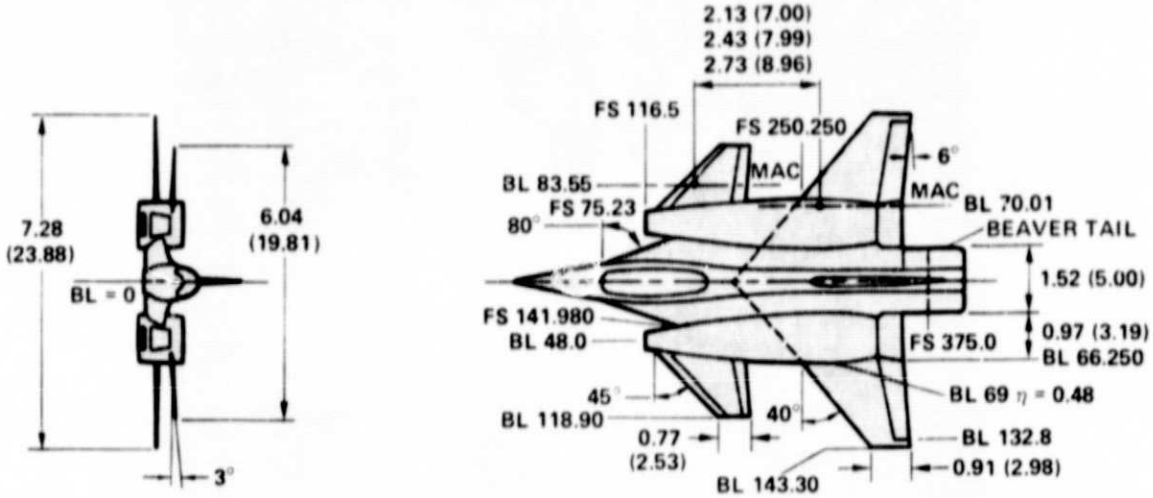

WING:

REFERENCE AREA, m^2 (ft^2)	17.00 (183.0)
ASPECT RATIO	3.12
TAPER RATIO	0.238
AIRFOIL SECTION	64A204
GEOMETRIC TWIST	-4°
MEAN AERO CHORD, m (ft)	2.33 (7.66)

CANARD:

AREA, m^2 (ft^2)	5.43 (58.5)
CANARD AREA/WING AREA	0.32
ASPECT RATIO	2.4
TAPER RATIO	0.345
AIRFOIL SECTION	64A004
MEAN AERO CHORD, m (ft)	1.51 (4.94)

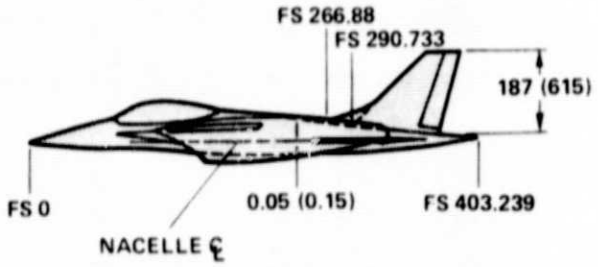

ALL DIMENSIONS IN m (ft)

(a) V/STOL fighter model overall geometry.

Figure 2.- V/STOL fighter model geometry.

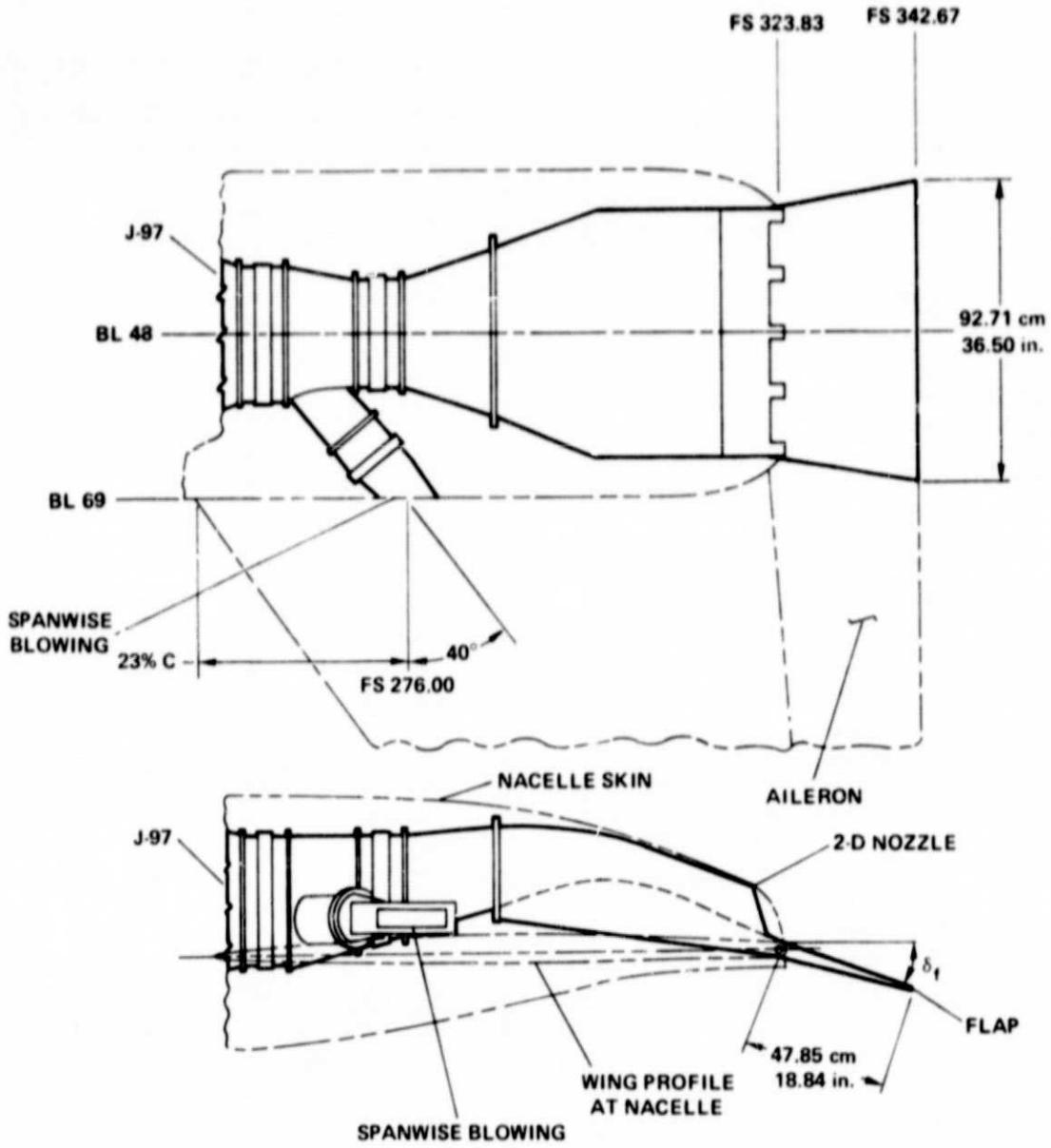

(b) Nozzle geometry.

Figure 2.- Concluded.

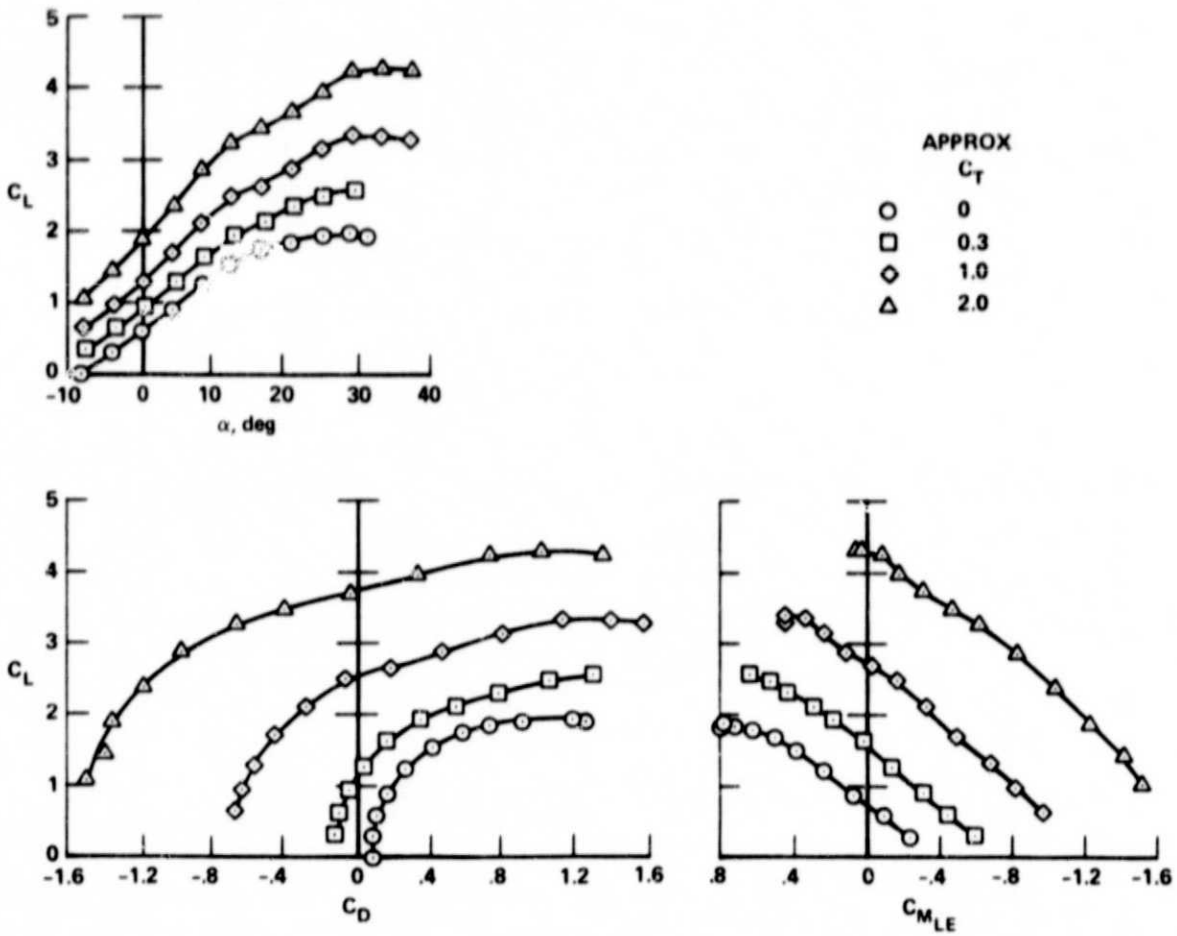

Figure 3.- Basic model longitudinal characteristics; $\delta_f = \delta_a = 30°$, $\delta_c = 0°$, SWB off.

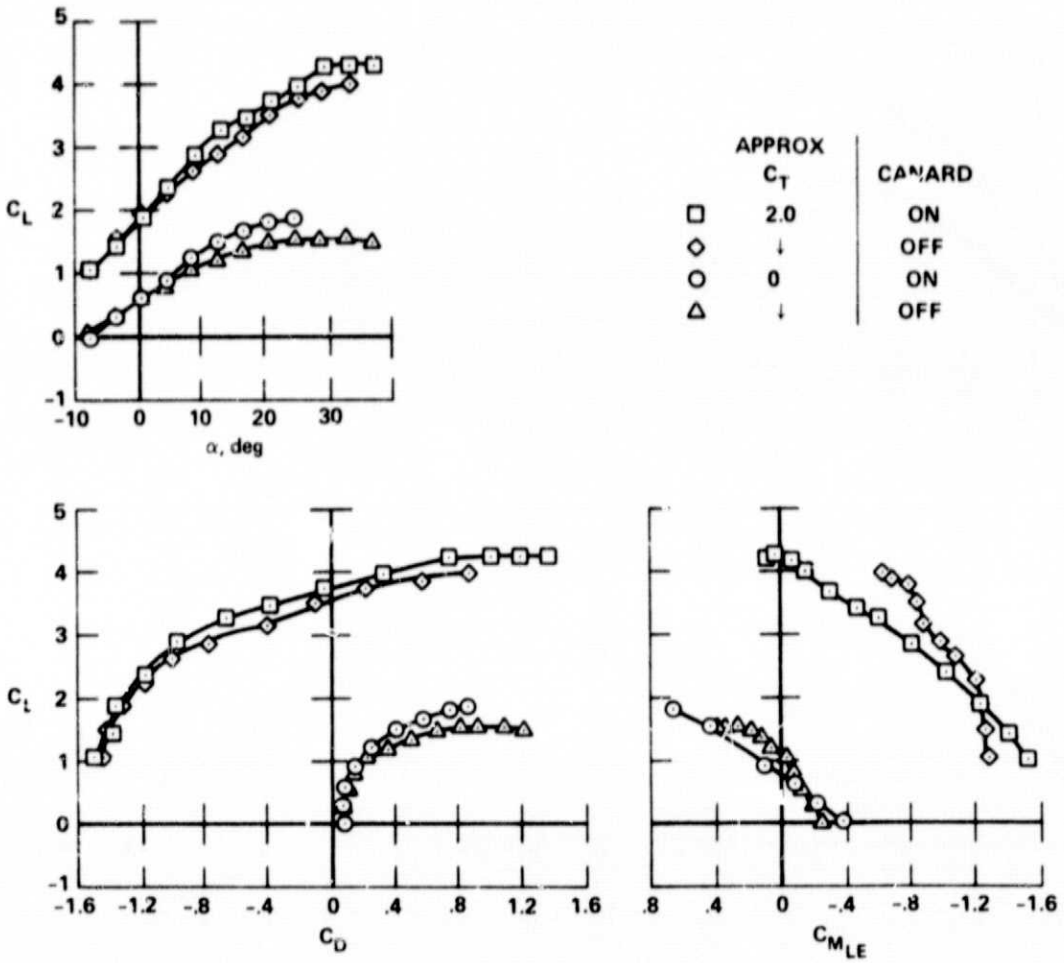

Figure 4.- Effect of canard on longitudinal characteristics; $\delta_f = \delta_a = 30°$, $\delta_c = 0°$, SWB off.

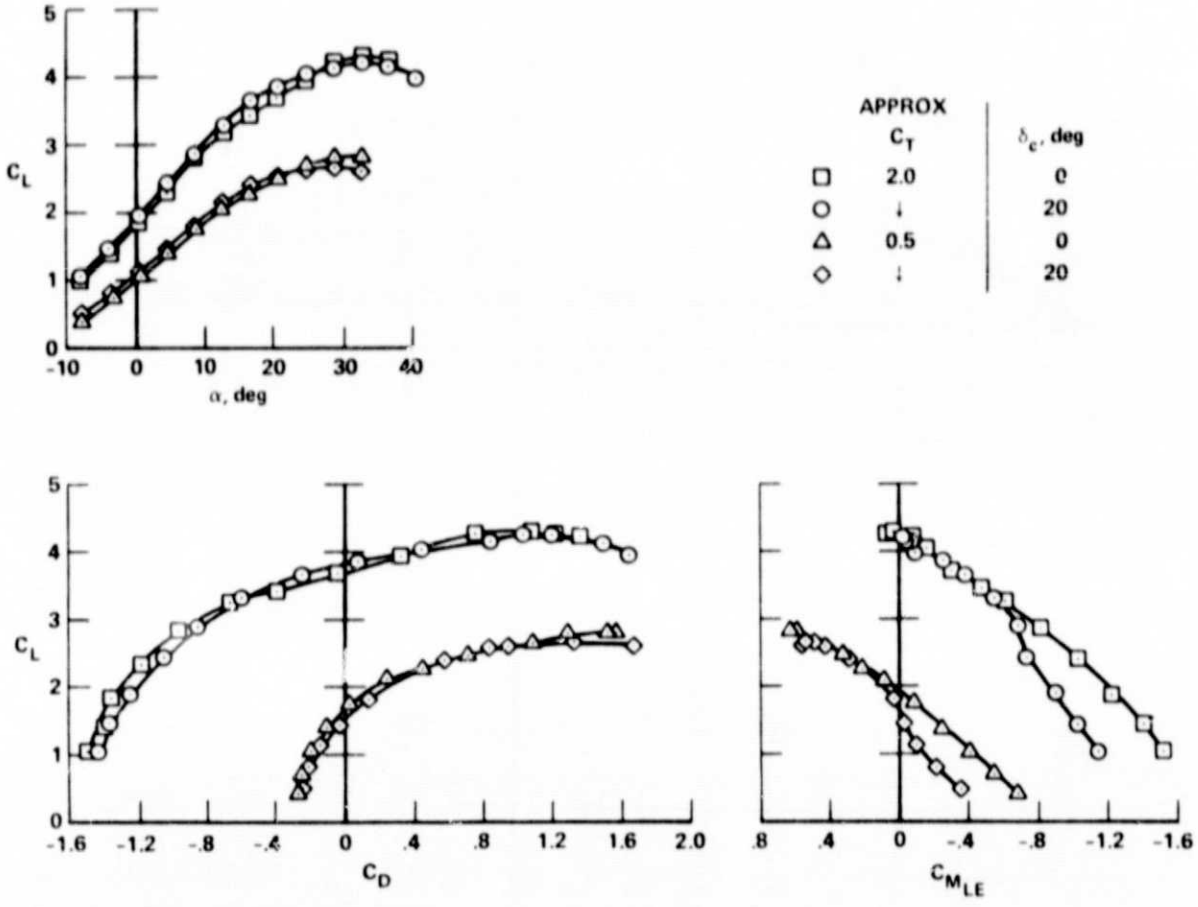

Figure 5.- Effect of canard deflection on longitudinal characteristics; $\delta_f = \delta_a = 30°$, SWB off.

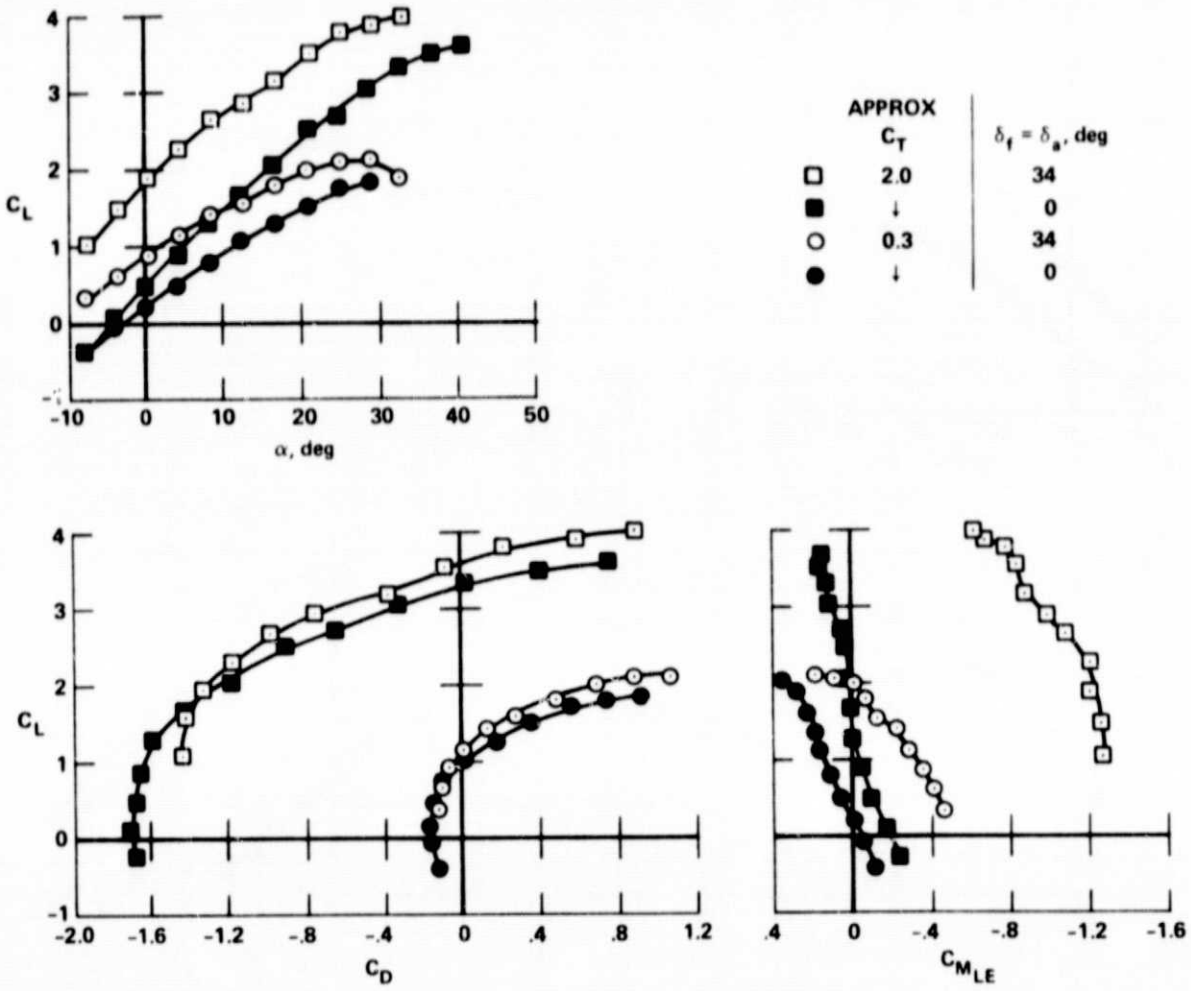

Figure 6.- Effect of flap/aileron deflection on longitudinal characteristics; canard and SWB off.

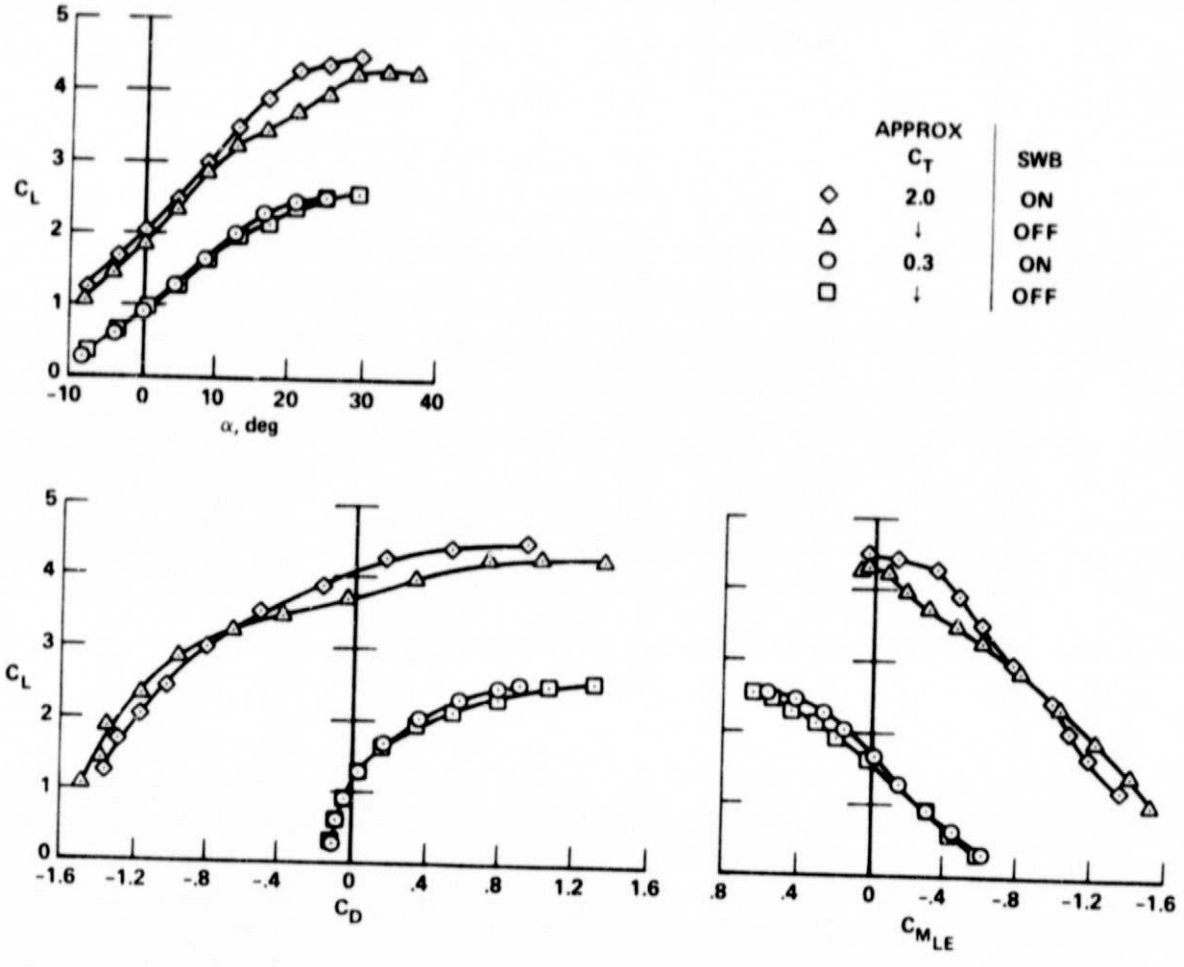

Figure 7.- Effect of spanwise blowing on longitudinal characteristics: $\delta_f = \delta_f = 30°$, $\delta_c = 0°$.

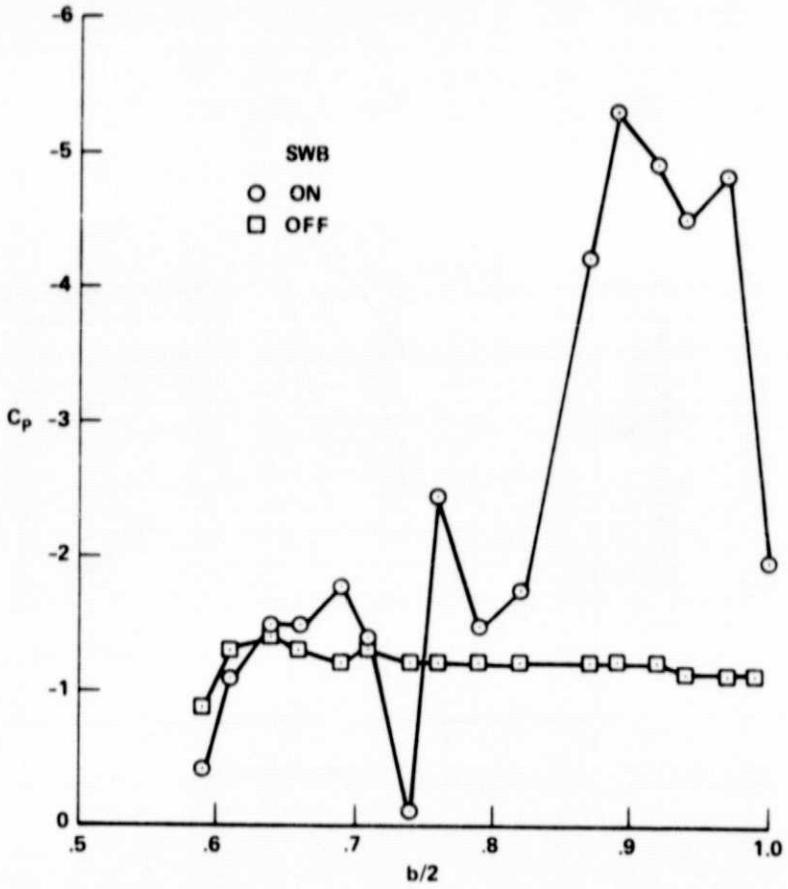

Figure 8.- Spanwise wing pressure distribution with and without SWB; $\delta_f = \delta_a = 30°$, $\delta_c = 0°$, $\alpha = 20°$, 0.50c.

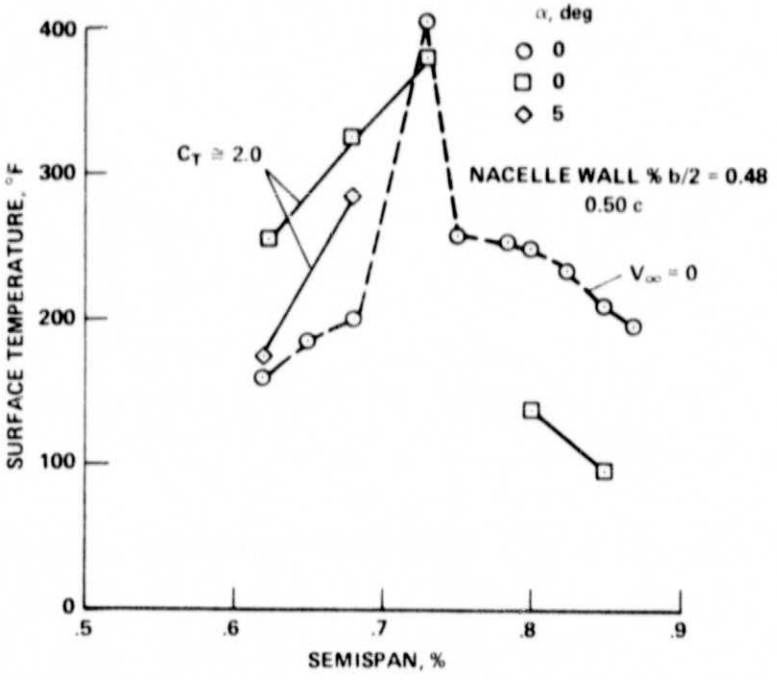

Figure 9.- Wing surface temperatures with SWB; $\delta_f = \delta_a = 30°$, $\delta_c = 0°$, $\alpha = 0°$.

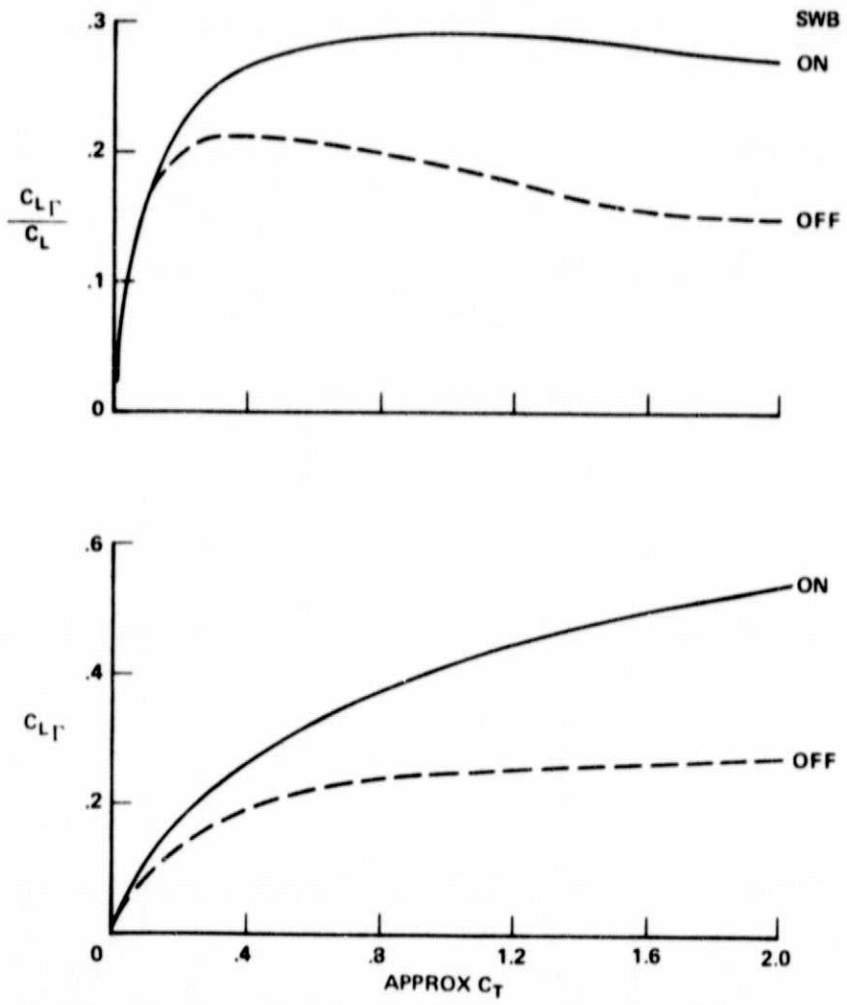

Figure 10.- Fighter model circulation lift; $\delta_f = \delta_a = 30°$, $\delta_c = 0°$, $\alpha = 0°$.

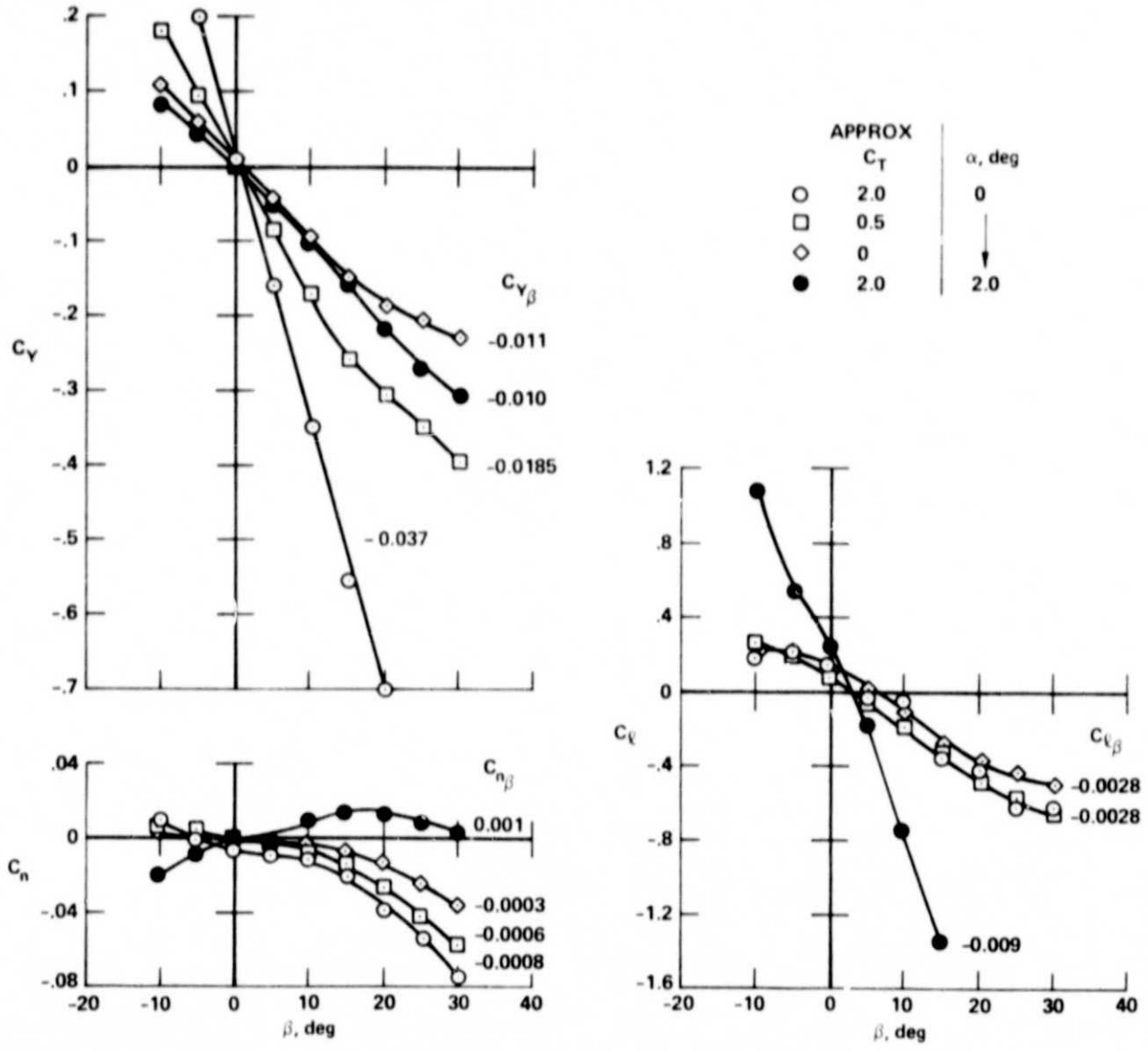

Figure 11.- Basic model lateral-direction characteristics; $\delta_f = \delta_a = 30°$, $\delta_c = 0$, SWB off.

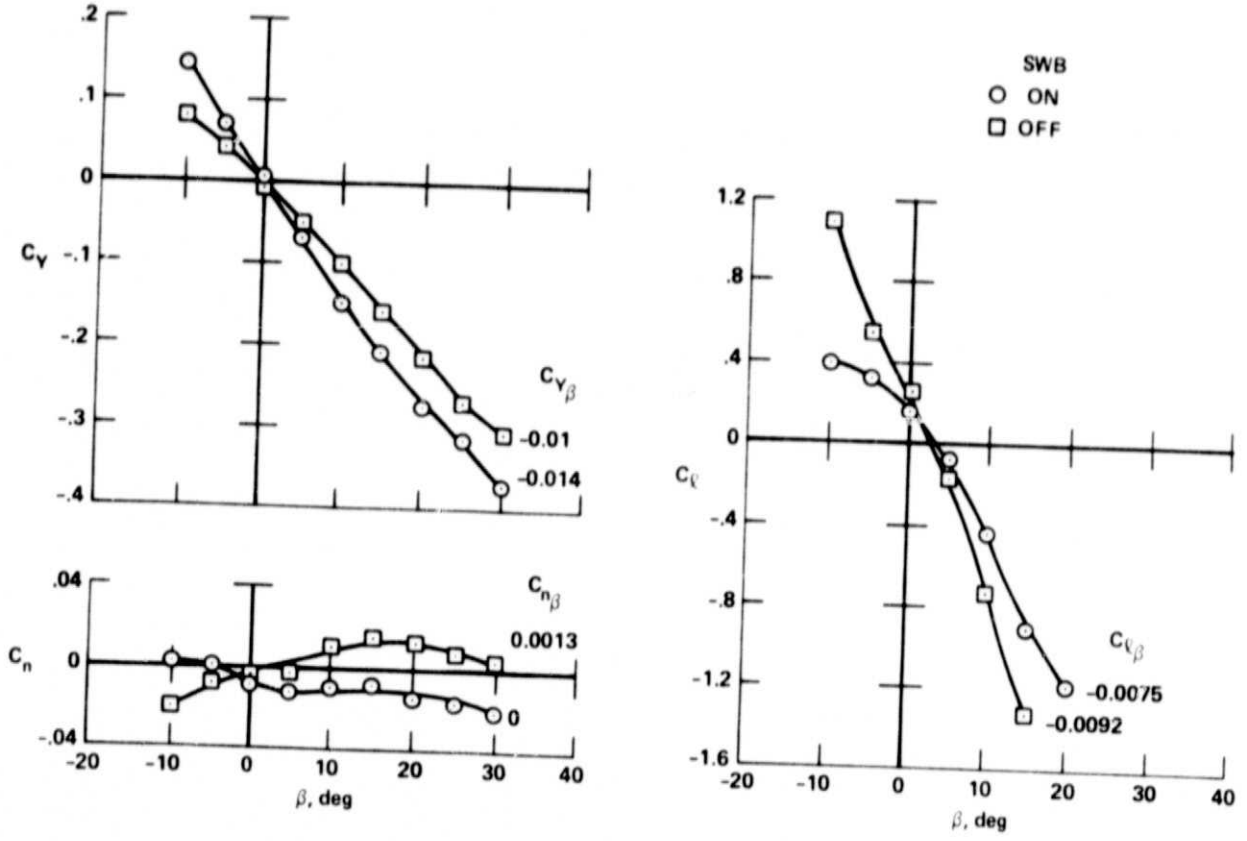

Figure 12.- Effect of SWB on lateral-directional characteristics; $\delta_f = \delta_a = 30°$, $\delta_c = 0°$, $\alpha = 0°$.